Materials and Design 46 (2013) 640–644

Contents lists available at SciVerse ScienceDirect

Materials and Design

journal homepage: www.elsevier.com/locate/matdes

The effect of cutting speed and heat treatment on the fatigue life of Grade 5 and Grade 23 Ti–6Al–4V alloys

W. Niu [a,b], M.J. Bermingham [a,b,*], P.S. Baburamani [c], S. Palanisamy [a,b], M.S. Dargusch [a,b], S. Turk [c], B. Grigson [c], P.K. Sharp [c]

[a] Defence Materials Technology Centre, School of Mechanical and Mining Engineering, The University of Queensland, Australia
[b] Queensland Centre for Advanced Materials Processing and Manufacturing (AMPAM), The University of Queensland, Australia
[c] Air Vehicles Division, Defence Science and Technology Organisation, Fishermans Bend, Victoria, Australia

ARTICLE INFO

Article history:
Received 6 August 2012
Accepted 30 October 2012
Available online 22 November 2012

Keywords:
Titanium alloys
Bulk deformation
Thermomechanical processing
Mechanical characterisation

ABSTRACT

High speed machining is a necessary manufacturing method for ensuring productivity and profitability. However, research has demonstrated that the high speed machining process impairs the surface characteristics of materials such as Ti–6Al–4V including surface roughness and subsurface microstructural damage. Therefore, there is concern that high speed machining detrimentally influences the fatigue properties of Ti–6Al–4V components. This paper investigates the effect of cutting speed on the surface integrity and fatigue properties of Ti–6Al–4V (ASTM Grade 5) and Ti–6Al–4V ELI (ASTM Grade 23) alloys in the beta annealed and mill annealed heat treated conditions. It was found that the surface roughness and fatigue properties are not significantly influenced by cutting speed, however, the microstructure substantially influences the properties.

1. Introduction

Titanium alloys are becoming more attractive due to their excellent mechanical properties, biocompatibility and corrosion resistance. In this manner, they are used in a wide range of applications in the aerospace, automotive, chemical and medical industries [1,2]. Except for a limited number of powder metallurgy products, most products fabricated from titanium alloys require machining processes [3]. Unfortunately, titanium alloys are 'difficult-to-machine' materials because of their low thermal conductivity and high reactivity with many cutting tool materials [4,5].

The fatigue of titanium alloys is of great concern because they are often used in critical applications such as fracture critical aircraft components. It is understood that a number of factors influence the fatigue properties of titanium alloys, including the microstructure [6–9], workpiece surface roughness [10–12] and post-surface treatment [13,14]. Naturally, the machining process can influence many of these factors [15–18] and therefore, the choice of machining parameters may ultimately influence the fatigue properties of the component.

Of all machining parameters, cutting speed is particularly important because it largely determines the material removal rate and manufacturing productivity. There is strong industrial desire and need to machine titanium alloys at high speed, and several technological developments have been made to enable high speed machining. These include new tooling developments, processing developments and machining strategies. Although these processes can permit faster cutting speeds, there is concern and uncertainty as to whether the cutting speed will affect the machined surface condition, the residual stress and the fatigue life of the component. Amin et al. have shown that increasing the cutting speed increases the machined surface roughness of titanium alloys [19], while others have found that cutting speed does not have a significant effect on surface roughness [20]. Increasing cutting speed is reported to also increase the subsurface microstructural variation [20]. The milling process is reported to generate compressive residual stress on the surface and this stress becomes more compressive with increasing cutting speed [20,21]. Therefore, higher cutting speeds may induce greater compressive residual stresses which may benefit the fatigue life by delaying crack nucleation/propagation; however, on the other hand, higher cutting speeds could result in increased surface roughness values that may assist with early crack nucleation and possibly reduce the fatigue life.

Although many authors have characterised the effect of cutting speed on residual stress or subsurface damage, there is essentially no literature that specifically investigates the effect of cutting speed on the fatigue of titanium alloys. The exception is the work of Geng and Xu [22] who report that the α-alloy TA15 is not microstructurally damaged during machining and this does not influence

* Corresponding author at: Defence Materials Technology Centre, School of Mechanical and Mining Engineering, The University of Queensland, Australia. Tel.: +61 733654147.
E-mail address: m.bermingham@uq.edu.au (M.J. Bermingham).

0261-3069/$ - see front matter © 2012 Elsevier Ltd. All rights reserved.
http://dx.doi.org/10.1016/j.matdes.2012.10.056

the fatigue life of the alloy. This is in contrast to much literature that reveals machining the α/β alloy Ti–6Al–4V significantly damages the microstructure near the machined surface [17,19,20,23]. Therefore, there is concern that the α/β Ti–6Al–4V may be susceptible to increased fatigue damage as a result of the machining process. Since Ti–6Al–4V is the most widespread titanium alloy used in the aerospace industry, there is a need to explore the effect of machining speed on the surface integrity, subsurface damage and fatigue life of components manufactured from this alloy. This paper will investigate these aspects on two commercial grades of titanium alloy Ti–6Al–4V (Grade 5) and Ti–6Al–4V Extra Low Interstitial (ELI) (Grade 23) in two common commercial heat treated conditions, Mill Annealed (MA) and Beta Annealed (BA).

2. Experimental details

The workpiece materials were alpha–beta titanium alloys, Ti–6Al–4V (ASTM Grade 5) and Ti–6Al–4V Extra Low Interstitial (ELI) (ASTM Grade 23) in Beta Annealed (BA) and Mill Annealed (MA) heat treatment conditions. The starting microstructure of each material used in this study is shown in Fig. 1. It is difficult to optically distinguish any difference between GR5 and GR23 for a given heat treatment because the slightly higher interstitial content of GR5 does not heavily influence the room temperature microstructure. In contrast, the heat treatment substantially influences the room temperature microstructure because during BA, the microstructure is largely determined by α-phase nucleation and growth processes on prior β-grain boundaries, whereas during MA the microstructure is determined largely by recrystallisation and grain growth processes. The MA heat treatment produces fine α-grains less than 50 μm long with intergranular β. Although the width is similar, the BA condition produces much longer α-grains that are usually clustered in colonies, again separated by intergranular β. These colonies have the same crystallographic orientation, and many colonies can form a single prior-β grain which is generally less than a millimetre in size [24].

To investigate the effect of cutting speed on fatigue life of the materials being investigated, coupons were machined at three different cutting speeds: 50, 100 and 150 m/min. The tool used for this study was JHP 750 HPM tribon end mill. Flood coolant was used during machining and the feed rate (0.04 mm/tooth) and depth of cut (2 mm) was kept constant. The geometry of the fatigue test coupon is shown in Fig. 2 and was selected according to the ASTM: E466-07. Table 1 gives the details of fatigue test coupons prepared. The experimental design aims to investigate the effect of cutting speed on the fatigue life of MA and BA GR5 and G23 alloys machined at different speeds. The experimental methods were selected because typical Ti–6Al–4V roughing speeds are about 50 m/min and typical finishing speeds are up to 150 m/min and MA and BA are common heat treatments used in industry for this alloy.

Three coupons were selected randomly for surface roughness measurements, using a MAHR Perthometer S3P with a Focodyn non-contact laser probe. The traverse length was 5.6 mm with a cut-off length of 0.8 mm.

Constant amplitude axial fatigue tests were carried out using a 250 kN servo-hydraulic Instron machine in load control mode, with a stress ratio $R(\sigma_{min}/\sigma_{max}) = 0.1$ and at a maximum stress of 600 MPa. The test frequency was 10 Hz. The tests were carried out at ambient temperature (21 ± 1 °C (69.8 ± 1.8 F)) and at a relative humidity of 40%. Three coupons were tested for each condition. The failure criterion was either a complete separation of specimen in the test section or the test reaching 10^6 cycles (run-out) without failure.

One coupon was cut perpendicular to the machined surfaces to carry out microhardness and microstructure tests. Standard metallographic sample preparation techniques were employed and Kroll's reagent (2 ml HF, 6 ml HNO_3, 92 ml H_2O) was used for

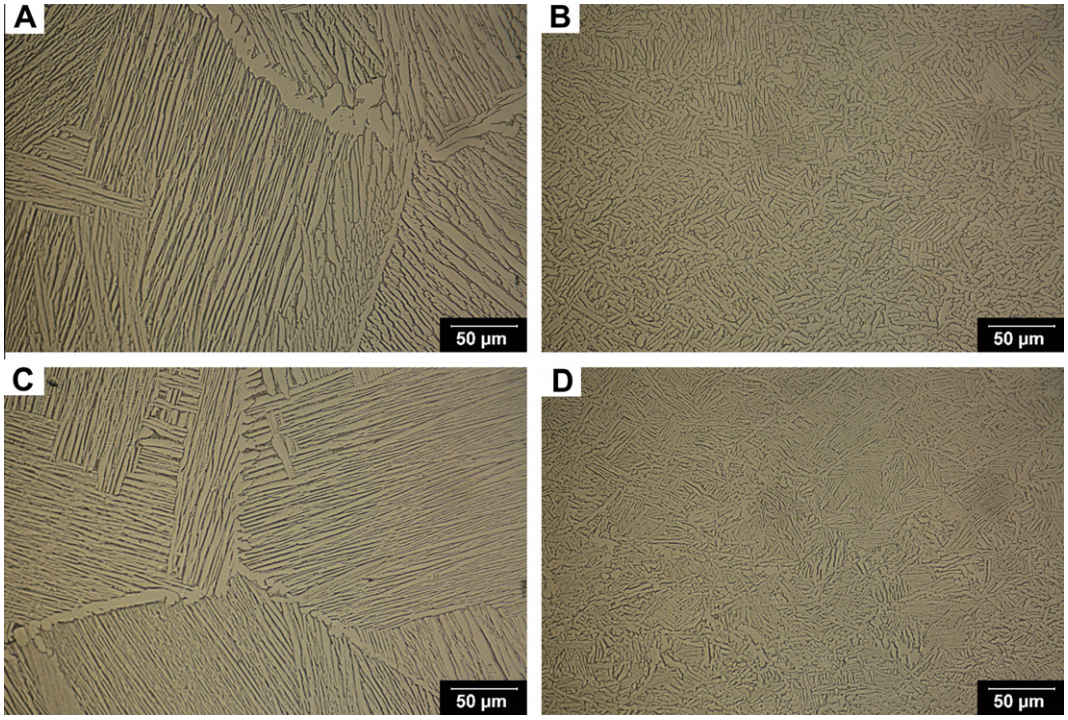

Fig. 1. Microstructures of starting material: (A) BA GR5; (B) MA GR5; (C) BA GR23; (D) MA GR23. There is no visible difference in the microstructures of GR5 and GR23 unless the heat treatment condition is changed. The BA heat treatment produces large colonies of α-grains that nucleate from prior-β grain boundaries. Each α-colony is comprised of multiple single α-laths that adopt the same crystallographic orientation. The MA heat treatment produces a much finer microstructure consisting of mostly individual α-laths/grains that adopt one of 12 possible crystallographic orientations, with very few α-colonies forming.

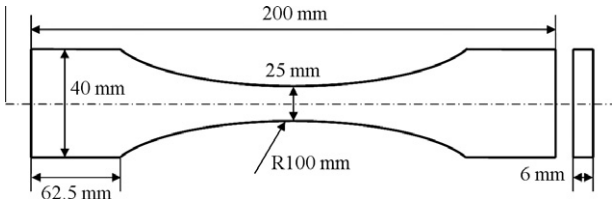

Fig. 2. Fatigue test coupon geometry. Not to scale.

Table 1
Details of fatigue test coupons manufactured.

Material	Heat treatment	Cutting speed (m/min)	Number of coupons
Ti–6Al–4V, GR5	MA	50, 100 and 150	5 per cutting speed
Ti–6Al–4V, GR5	BA	100	5
Ti–6Al–4V, GR23	BA	50, 100 and 150	5 per cutting speed
Ti–6Al–4V, GR23	MA	100	5

microscope examination [25]. Microhardness was measured from the surface to a depth up to 300 μm with a load of 10 g for 12 s.

3. Results and discussion

The surface roughness usually plays a key role on fatigue life because cracks generally initiate from free surfaces [12]. Fig. 3 shows the mean surface roughness values of the machined GR5 and GR23 titanium alloys. The surface roughness for all samples was between 0.29 μm and 0.44 μm. The error bars represent a standard deviation indicating some variation in the data. To help determine if statistical differences exist between each data set, one-way ANOVA and Tukey's multi-comparison test with 0.05 significance was applied. This method compares the means of each data set and determines whether a significant difference exists with 95% level of confidence. Details of this test are widely available in the literature (e.g. [26]). The results of this analysis are summarised in Table 2.

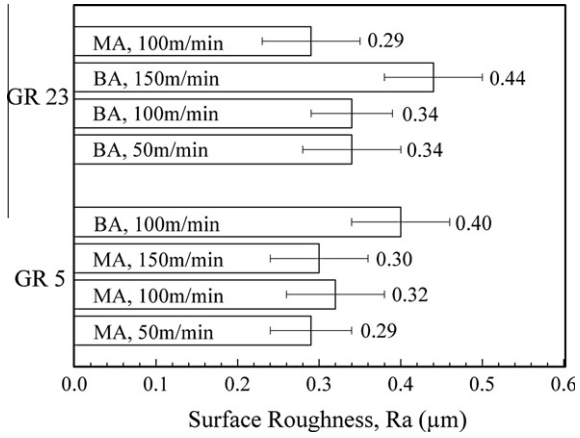

Fig. 3. Surface roughness for each material. The error bars indicate ±1 standard deviation.

A few trends are apparent in this analysis. Firstly, there is no statistical difference in surface roughness for any MA condition, including changes to cutting speeds or alloy type. The same conclusion can be made about the GR23 BA condition up to 100 m/min, however, at 150 m/min the surface roughness is found to be statistically larger than at lower speeds. With the exception of G23BA 150 m/min, it appears that the surface roughness values are not affected by cutting speed when machining either alloy. In addition, the MA condition has lower mean surface roughness than the BA condition, when machining Ti–6Al–4V at those cutting speeds investigated.

Fig. 4 shows the typical microstructure of the BA and MA samples machined at 100 m/min. The microstructure near the machined surface reveals some damage associated with machining. The α-grains in the BA material are deformed at the surface and 'bend' in the direction of the cutter, to a depth of approximately 5–15 μm below the surface. This phenomenon is most obvious when the cutting direction is perpendicular to the growing direction of the α-grain colony, and occurs in both GR5 and G23 material. The α-grains in the MA material appear to experience little, if any, visible deformation near the surface.

The microhardness below the machined surface was measured to assess the extent of subsurface deformation from the machining process. This method is often used to identify subsurface damage and is a strong indication of machining induced strain hardening [27]. The microhardness results are presented in Fig. 5. At 100 m/min, both GR5 BA and GR23 BA conditions exhibit a hardened region of material directly below the machining surface to a depth of around 100 μm, with the highest hardness found nearest to the surface. This hardness profile rapidly decreases to the bulk hardness value of the material as the distance from the surface is increased. The MA condition for GR5 and GR23 did not display a clear hardened zone near the surface. This supports the visual evidence that the MA microstructure is relatively undamaged in comparison with the BA microstructure. However, it is also clear that the subsurface damage extends beyond that optically observed in the microstructures. For example, in Fig. 4 the depth of visible plastic deformation extents to approximately 15 μm, however, the microhardness results indicate hardening extends much deeper, up to approximately 100 μm. This hardening is most likely attributed to strain hardening

Table 2
Summary of the Tukey multi-comparison test at 95% significance for surface roughness. 'No' indicates that the means are not statistically significant, 'Yes' indicates that the means are statistically different.

		GR5				GR23			
		MA,50	MA,100	MA,150	BA,100	BA,50	BA,100	BA,150	MA,100
GR5	MA,50	-	No	No	Yes	Yes	Yes	Yes	No
	MA,100		-	No	Yes	No	No	Yes	No
	MA,150			-	Yes	Yes	Yes	Yes	No
	BA,100				-	Yes	Yes	Yes	Yes
GR23	BA,50					-	No	Yes	Yes
	BA,100						-	Yes	Yes
	BA,150							-	Yes
	MA,100								-

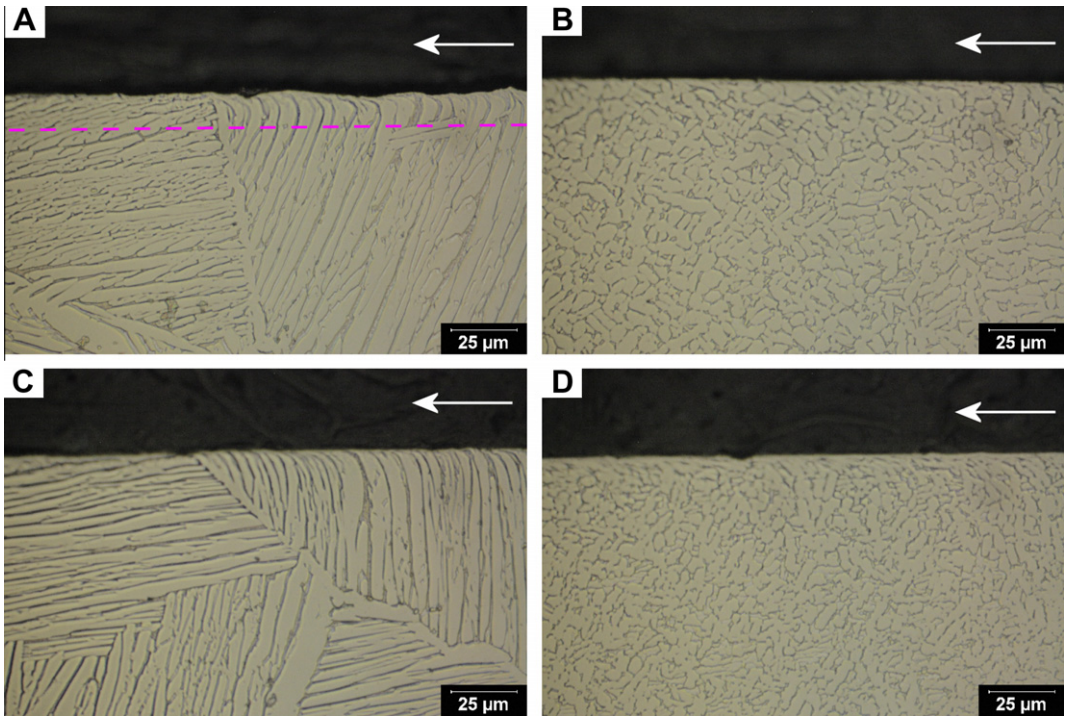

Fig. 4. Microstructures of (A) GR5 BA, (B) GR5 MA, (C) GR23 BA and (D) GR23 MA machined at 100 m/min. The white arrow indicates the cutting direction. At the machined surface, the cutter plastically deforms the microstructure. This is best observed in the BA microstructures that contain elongated α-grains perpendicular to the cutting direction. In both (A) and (C) elongated α-grains appear to bend at almost 90°. The dashed line in (A) provides an example of the extent of plastic deformation: below approximately 5–15 μm from the surface it is difficult to optically detect plastic deformation induced by machining. Optically, the MA microstructures appear to be less damaged.

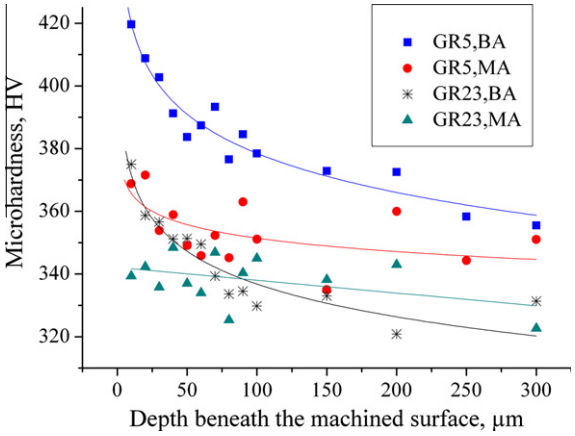

Fig. 5. Microhardness of GR5 and GR23 alloys machined at 100 m/min. The presented data is the average value of nine individual points at the same depth.

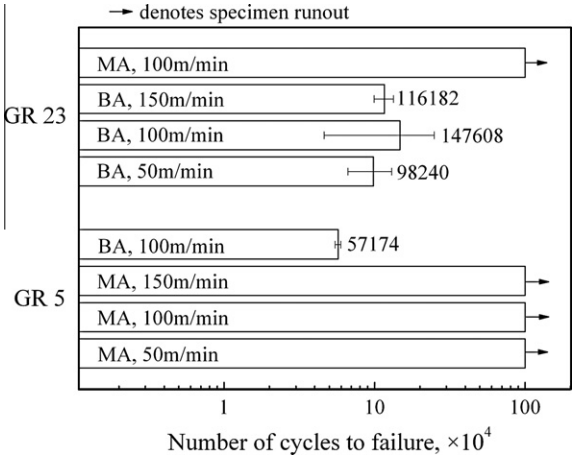

Fig. 6. Mean fatigue life of various materials. Some specimens failed in the grip section of the test coupon and were omitted, however, the results presented are the average of at least three valid tests per condition. Testing was stopped after about 10^6 cycles (run-out).

and confirms that microhardness measurements are more appropriate in detecting machining damage than optical examination of the microstructures alone. The increase of hardness leads to the increase of tensile stress whilst decreasing the ductility and impact values. Therefore, the work hardened surface may have an effect on the fatigue behaviour (crack initiation and propagation) [28] of GR23 material. In addition, it can be seen that GR5 alloys have slightly higher hardness values than GR23 alloy (ELI grade) under each heat treatment condition because of higher oxygen content.

Fig. 6 shows the mean fatigue life for all specimens. In all cases, run-out occurred for the MA materials regardless of which cutting speed was used, indicating a fatigue life greater than 10^6 cycles. In contrast, all BA materials experienced fatigue failure between 50,000 and 150,000 cycles. Despite their apparent variation, the mean fatigue life variation for all BA materials under different cutting speeds is not significant (95% confidence) using the same ANOVA multi-comparison test as that performed for surface roughness (the results are summarised in Table 3). This indicates that the cutting speed has no measurable influence on the fatigue life of GR23 BA and GR5 MA alloys, for the test parameters used in this study. The only factor that appears to influence the fatigue properties is the heat treatment condition, particularly the grain size, after mill annealing and beta annealing.

From the surface roughness results (Fig. 3), the MA specimens were found to have lower mean surface roughness than the BA samples and this will help reduce the crack initiation from the

Table 3
Summary of the Tukey multi-comparison test at 95% significance for fatigue testing. 'No' indicates that the means are not statistically different. All BA means are statistically different from all MA means (not included in this table).

	GR5 BA,100	GR23 BA,50	GR23 BA,100	GR23 BA,150
GR5 BA,100	-	No	No	No
GR23 BA,50		-	No	No
GR23 BA,100			-	No
GR23 BA,150				-

surface. However, the surface roughness cannot be exclusively linked to fatigue life in this work because there is no statistical difference between the surface roughness of some BA and MA alloys, yet, the MA alloys all have a far greater fatigue life than the BA alloys. For example, the GR5 MA, 100 m/min sample with 0.32 μm roughness had a fatigue life greater than 10^6 cycles, whereas the GR23 BA, 50 m/min and GR23 BA, 100 m/min had a similar roughness of 0.34 μm but a lower fatigue life of 147,608 cycles.

Instead, the high fatigue life of MA specimens can be attributed to the heat treatment method and the resultant microstructure and grain size. It is reported that MA heat treatment retards crack initiation rates as much as two times compared to BA [29]. Although MA increases crack growth rate to some extent [30], it is still not significant during this fatigue testing because high cycle fatigue is often dominated by crack nucleation [29]. The fact that the small equiaxed MA microstructure produced superior fatigue life compared to the large grained BA microstructure is expected considering that fatigue life is reported to be grain size dependent and follow a Hall–Petch relationship [7,31]. Evans also demonstrated that fine grained MA microstructures produce superior fatigue life compared to coarse grained BA microstructures [32].

Despite the presence of subsurface deformation and variations to surface finish, the presented work indicated that machining up to a cutting speed of 150 m/min is unlikely to influence the fatigue properties of Ti–6Al–4V components. This is encouraging for manufacturing centres that wish to adopt cutting speeds up to 150 m/min in their machining strategies to produce Ti–6Al–4V components.

4. Conclusions

The effect of cutting speed on the surface roughness and fatigue life of Ti–6Al–4V (Grade 5) and Ti–6Al–4V ELI (Grade 23) alloys in beta-annealed and mill-annealed conditions was investigated at a stress level of 600 MPa. For the stress level tested (i.e. 600 MPa) and cutting speeds (50 m/min, 100 m/min and 150 m/min) investigated, a summary of the key findings are:

- No clear relationship can be found between cutting speed and surface roughness for either alloy machined at surface speeds between 50 m/min and 150 m/min.
- The MA condition appears less susceptible to surface damage associated with machining and had lower surface roughness than the BA condition.
- Cutting speed, within the test range (50–150 m/min) has no measurable influence on the fatigue life of either alloy.
- The MA heat treatment leads to significantly longer fatigue life than the BA heat treatment. This was attributed to general microstructural effects including a grain size-fatigue property relationship rather than surface roughness.

Acknowledgements

The authors would also like to acknowledge the support of the Defence Materials Technology Centre (DMTC) and the Queensland Centre for Advanced Materials Processing and Manufacturing (AMPAM). The DMTC was established and is supported under the Australian Government's Defence Future Capability Technology Centres Programme. The authors also would like to acknowledge the support of the Australian Defence Science and Technology Organisation (DSTO).

References

[1] Yang X, Richard Liu C. Machining titanium and its alloys. Mach Sci Technol 1999;3:107–39.
[2] Chunxiang C, BaoMin H, Lichen Z, Shuangjin L. Titanium alloy production technology, market prospects and industry development. Mater Design 2011;32:1684–91.
[3] EO E. Key improvements in the machining of difficult-to-cut aerospace superalloys. Int J Mach Tool Manuf 2005;45:1353–67.
[4] Jawaid A, Che-Haron CH, Abdullah A. Tool wear characteristics in turning of titanium alloy Ti-6246. J Mater Process Technol 1999;92–93:329–34.
[5] Bhaumik SK, Divakar C, Singh AK. Machining Ti–6Al–4V alloy with a wBN–cBN composite tool. Mater Design 1995;16:221–6.
[6] Eylon D, Pierce C. Effect of microstructure on notch fatigue properties of Ti–6Al–4V. Metall Mater Trans A 1976;7:111–21.
[7] Nakajima K, Terao K, Miyata T. The effect of microstructure on fatigue crack propagation of α+β titanium alloys: in-situ observation of short fatigue crack growth. Mater Sci Eng A 1998;243:176–81.
[8] Mall S, Namjoshi SA, Porter WJ. Effects of microstructure on fretting fatigue crack initiation behavior of Ti–6Al–4V. Mater Sci Eng A 2004;383:334–40.
[9] Zuo JH, Wang ZG, Han EH. Effect of microstructure on ultra-high cycle fatigue behavior of Ti–6Al–4V. Mater Sci Eng A 2008;473:147–52.
[10] Bentley SA, Mantle AL, Aspinwall DK. The effect of machining on the fatigue strength of a gamma titanium aluminide intermetallic alloy. Intermetallics 1999;7:967–9.
[11] Sharman ARC, Aspinwall DK, Dewes RC, Clifton D, Bowen P. The effects of machined workpiece surface integrity on the fatigue life of γ-titanium aluminide. Int J Mach Tool Manuf 2001;41:1681–5.
[12] Novovic D, Dewes RC, Aspinwall DK, Voice W, Bowen P. The effect of machined topography and integrity on fatigue life. Int J Mach Tool Manuf 2004;44:125–34.
[13] Drechsler A, Kiese J, Wagner L. Effects of shot peening and roller-burnishing on fatigue performance of various titanium alloys. The 7th International Conference on Shot Peening (ICSP7), Warsaw Poland; 1999. p. 145–152.
[14] Zhang XC, Zhang YK, Lu JZ, Xuan FZ, Wang ZD, Tu ST. Improvement of fatigue life of Ti–6Al–4V alloy by laser shock peening. Mater Sci Eng A 2010;527:3411–5.
[15] Sharman ARC, Aspinwall DK, Dewes RC, Bowen P. Workpiece surface integrity considerations when finish turning gamma titanium aluminide. Wear 2001;249:473–81.
[16] Ezugwu EO, Bonney J, Da Silva RB, Çakir O. Surface integrity of finished turned Ti–6Al–4V alloy with PCD tools using conventional and high pressure coolant supplies. Int J Mach Tool Manuf 2007;47:884–91.
[17] Che-Haron CH, Jawaid A. The effect of machining on surface integrity of titanium alloy Ti–6% Al–4% V. J Mater Process Technol 2005;166:188–92.
[18] CH C-H. Tool life and surface integrity in turning titanium alloy. J Mater Process Technol 2001;118:231–7.
[19] Amin AKMN, Ismail AF, Nor Khairusshima MK. Effectiveness of uncoated WC–Co and PCD inserts in end milling of titanium alloy—Ti–6Al–4V. J Mater Process Technol 2007;192–193:147–58.
[20] Sun J, Guo YB. A comprehensive experimental study on surface integrity by end milling Ti–6Al–4V. J Mater Process Technol 2009;209:4036–42.
[21] Sridhar BR, Devananda G, Ramachandra K, Bhat R. Effect of machining parameters and heat treatment on the residual stress distribution in titanium alloy IMI-834. J Mater Process Technol 2003;139:628–34.
[22] Geng GS, Xu JH. Surface integrity and fatigue property of a high speed milled titanium alloy. Adv. Mater. Res. 2008;53–54:305–10.
[23] Thomas M, Turner S, Jackson M. Microstructural damage during high-speed milling of titanium alloys. Scripta Mater 2010;62:250–3.
[24] Germain L, Gey N, Humbert M. Reliability of reconstructed β-orientation maps in titanium alloys. Ultramicroscopy 2007;107:1129–35.
[25] Vander Voort GF. Metallography principles and practice. New York: McGraw-Hill; 1984.
[26] Ramsey P, Ramsey, P. Tukey-Kramer procedure. In: Salkind N, editor. Encyclopedia of measurement and statistics. Thousand Oaks, CA: SAGE Publications, Inc; 2007. p. 1017–20.
[27] Ulutan D, Ozel T. Machining induced surface integrity in titanium and nickel alloys: a review. Int J Mach Tool Manuf 2011;51:250–80.
[28] Wagner L, Gregory JK. Thermomechanical surface treatment of titanium alloys. Int J Fatigue 1995;17:448.
[29] Boyer R, Welsch G, Collings EW. Materials properties handbook – titanium alloys. ASM Int 1994;2(1):44–55.
[30] Matthew J, Donachie J. Titanium a technical guide. 2nd ed. ASM International; 2000.
[31] Morita T, Takahashi H, Shimizu M, Kawasaki K. Factors controlling the fatigue strength of nitrided titanium. Fatigue Fract Eng Mater Struct 1997;20:85–92.
[32] Evans WJ. Microstructure and the development of fatigue cracks at notches. Mater Sci Eng A 1999;263:160–75.